

**CAI PRECURSOR COMPOSITIONS COMPUTED FROM SI AND MG ISOTOPE MEASUREMENTS.**

D.S. Ebel<sup>1</sup>, F.M. Richter<sup>2</sup>, and E.D. Young<sup>3</sup>. American Museum of Natural History, New York, NY <sup>2</sup>The University of Chicago, Chicago, IL 60637, USA. <sup>3</sup> University of California Los Angeles, Los Angeles, CA 90095. (del@amnh.org)

**Introduction:** Calculations of the composition of materials that condense in chemical equilibrium with a vapor of solar composition as a function of decreasing temperature at constant  $P(H_2)$  [1] provide a baseline with which to address the origin and evolution of primitive refractory inclusions in meteorites. However, a serious problem arises in that calculated condensates contain solar proportions of  $CaO/Al_2O_3=0.792$  (wt%) before appreciable silicon and magnesium condense, while actual Ca- Al-rich inclusions (CAIs) have  $CaO/Al_2O_3$  values ranging from  $\sim 0.5$  to  $\sim 1.2$  [2]. A second problem is that many inclusions such as most Type B CAIs from CV3 chondrites are depleted in MgO compared to the expectation based on condensation calculations.

The relative depletion in MgO, and very likely  $SiO_2$  as well, of the Type B CAIs compared to calculated condensates can be explained as resulting from condensate precursors having been reheated for a sufficiently long time that measurable amounts of Si and Mg were lost by evaporation [3]. Partial evaporation also explains the common observation that the Type B CAIs are enriched in the heavy isotopes of Si and Mg in much the same way as evaporation residues produced in the laboratory [4]. These experiments also show that partial evaporation does not measurably fractionate the highly refractory elements calcium and aluminum at temperatures below  $\sim 2100$  K.

The most likely explanation for the variable, non-solar bulk  $CaO/Al_2O_3$  ratios (wt%) reported for coarse-grained CAIs is that reported compositions are derived from INAA measurements often of small fragments of an inclusion, or by modal mapping of a single plane surface through a heterogeneous three dimensional object. The implication, that after more than forty years of studying coarse-grained CAIs their true bulk compositions are still not well determined is profoundly troubling. Any independent way to better constrain CAI compositions would be a very valuable contribution.

**Conceptual Framework:** Shahar and Young used isotopes to constrain the Si/Mg ratio of the precursor [5], following their suggestion that the Mg and Si isotopic compositions of a CAI are sufficient to determine the abundance of MgO and  $SiO_2$  of the precursor [6]. They calculated Mg and Si isotopic evolution by evaporation of potential precursors to find which best fits the measured isotopic composition of a given CAI.

This approach requires a robust method for calculating trajectories in  $SiO_2$ -MgO space of the evolving evaporation residues and also knowledge of the kinetic isotope fractionation factors necessary for calculating the isotopic evolution of the residues. Bulk composition evolves based on the evaporation flux of Mg,  $J_{MgO}$ , and Si,  $J_{SiO_2}$ , given by:

$$J_{MgO} = \gamma_{Mg} P_{Mg}^{sat} / \sqrt{2\pi m_{Mg} RT}$$

$$J_{SiO_2} / J_{MgO} = (\gamma_{Si} P_{SiO}^{sat} / \gamma_{Mg} P_{Mg}^{sat}) \sqrt{m_{SiO} / m_{Mg}}$$

Thermodynamic models of gas speciation and liquid oxide activities [7] are required to determine the dominant gas species of mass  $m_{Mg}$  and  $m_{SiO}$  in equilibrium with the melt and their saturation vapor pressures  $P_{Mg}^{sat}$  and  $P_{SiO}^{sat}$ . Evaporation coefficients  $\gamma_{Mg}$  and  $\gamma_{Si}$  are empirically determined by vacuum evaporation experiments [4]. Once one has calculated the evaporation trajectory for each potential precursor, the associated trajectory in magnesium and silicon isotopic space is calculated using the Rayleigh equation  $R = R_o F_i^{(\alpha_i - 1)}$  where  $R$  is the isotopic ratio (e.g.  $^{25}Mg/^{24}Mg$ ) of a residue with initial ratio  $R_o$  that has a fraction  $F_i$  of the original abundance of the isotope in the denominator of  $R$ . The quantities  $\alpha_i$  are kinetic isotope fractionation parameters derived from laboratory evaporation experiments [4].

In principle, bulk CaO and  $Al_2O_3$  compositions in CAIs can also be estimated, because the activities of MgO and  $SiO_2$  in CAI melts are sensitive to composition. Here, calculations assume a wt% ratio of  $CaO/Al_2O_3=1.142$ .

**Case 1: Finding the Precursor of Laboratory-Produced Evaporation Residues.** Here we use model calculations to determine the starting compositions that (when evaporated) reproduce the silicon and magnesium isotopic composition [8] of a series of residues evaporated in vacuum at  $T=2073K$ . For this test, we use previously published values of  $\gamma_{Mg}=\gamma_{Si}$ ,  $\alpha_{Mg}=0.9871$  and  $\alpha_{Si}=0.990$  [4, 9]. Figure 1 shows the starting compositions investigated and the field of  $SiO_2$ -MgO space of the evaporation trajectories. Figure 2 shows the corresponding field of solutions in  $\delta^{29}Si$ - $\delta^{25}Mg$  space along with the measured isotopic composition of three laboratory evaporation residues.

Figure 3 shows the starting compositions that match the silicon and magnesium isotopic composition of the laboratory residues along with the actual starting composition (i.e., the precursor) for the laboratory experiments.

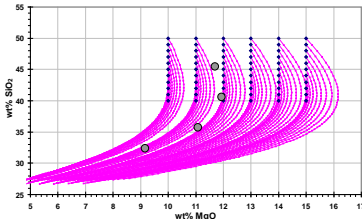


Fig. 1: Case 1 composition trajectories.

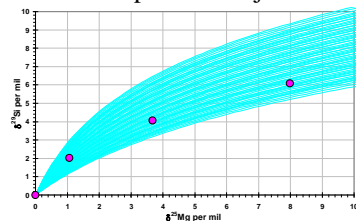


Fig. 2: Case 1 isotopic fractionation trajectories.

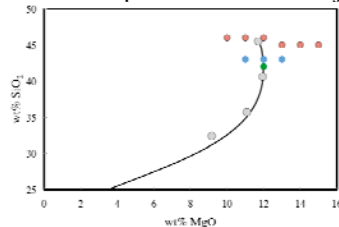


Figure 3. Precursors that have trajectories in isotope space that match the sample data to within  $\pm 0.05\text{‰}$ . The red (blue, green) symbols are possible precursors for the least, moderately, and most fractionated samples. The gray symbols show the composition of the residues and the continuous curve is the calculated trajectory for the starting composition of these samples.

**Case 2: Finding the Precursor of CAIs:** Here we use silicon and magnesium isotopic compositions of CAIs reported in various sources [10,11, 12] to attempt to reconstruct their possible precursors. For this case we assume the evaporation temperature was 1723K (a reasonable super-liquidus temperature for a Type B CAI composition). For this lower temperature than case 1, we adopt values  $\gamma_{Mg}=0.5 \cdot \gamma_{Si}$ ,  $\alpha_{Mg}=0.990$  and  $\alpha_{Si}=0.990$  [4, 9].

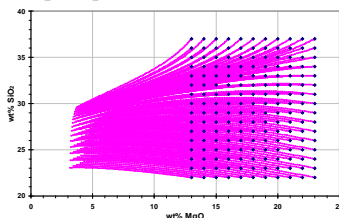


Fig. 4: Case 2 composition trajectories.

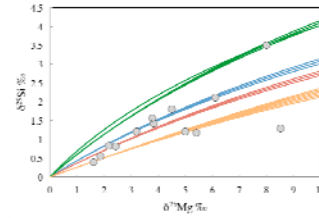


Fig. 5: Case 2, selected isotopic fractionation trajectories that fit within  $0.1\text{‰}$  all but one of the CAI isotopic compositions

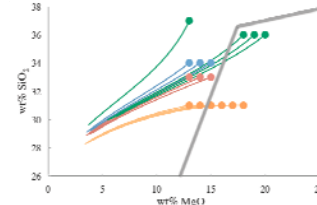


Fig. 6: Precursor compositions that have trajectories in isotope space that fit the CAI data to within  $\pm 0.1\text{‰}$ . Color code as in Fig. 5. The gray line is a portion of the equilibrium condensation trajectory of a vapor of solar composition at  $10^{-3}$  bars total pressure.

- Conclusions:**
1. The Si and Mg isotopic composition of evaporation residues can be used to determine lines in composition space that fall reasonably close to their precursor composition. The lengths of these lines decrease as the isotopic fractionations become larger
  2. The accuracy of the method is very sensitive to the value of kinetic parameters  $\gamma$  and  $\alpha$ .

3. Estimated precursor compositions in Case 1 can be improved by selecting a value of  $\gamma_{Mg}/\gamma_{Si}$  that results in a better fit of the composition trajectory to that of the residues.

4. Case 2 resulted in estimates of the composition of precursors to actual CAIs that are reasonably close to a condensation trajectory for a vapor of solar composition at  $10^{-3}$  bars total pressure.

**References:** [1] Grossman L (1972) *GCA* 36, 597-619. [2] Simon SB, Grossman L (2004) *GCA* 68, 4237-4248. [3] Grossman L et al., (2000) *GCA* 64, 2879-2894. [4] Richter FM (2007) *GCA* 71, 5544-5564. [5] Young ED, Shahar A (2010) *LPS* 2010 abs. #1551. [6] Shahar A and Young ED (2007) *EPSL* 257, 497-510. [7] Ebel DS and Grossman L (2000) *GCA* 64, 339-366. [8] Janney P et al., (2010) *in press Chem Geol*. [9] Knight K et al. (2009) *GCA* 73, 6390-6401. [10] Grossman L et al. (2008) *GCA* 72, 3001-3021. [11] Knight K et al. (2009) *LPSC XV* abs. #2360 [12] Bullock ES et al. (2010) *MaPS Suppl.* 45, A26, abs. #5364.